npj | vaccines

Article

Published in partnership with the Sealy Institute for Vaccine Sciences

https://doi.org/10.1038/s41541-026-01424-w

Evaluating varicella-zoster virus vaccine immunogenicity through Fc-mediated antibody functions: the roles of ADCP and ADCC

Check for updates

Sivilay Xayaheuang[1], Ji-Young Hwang[1], Yunhwa Kim[1], Kyung-Min Lee[1], Seok-Tae Choi[1], Eun-Jeong Jang[1], Ji-Soo Lim[2], Ji Young Bang[3], Han Sol Lee[4], Ok Sarah Shin[2,5], Ji Yun Noh[6], So-Hee Hong[3] & Hosun Park[1,7] ✉

Assessing the functional activity of vaccine-induced antibodies is critical for evaluating immunogenicity. We developed and validated antibody-dependent cellular phagocytosis (ADCP) and antibody-dependent cellular cytotoxicity (ADCC) assays to quantify Fc-mediated antibody responses elicited by varicella and zoster vaccines. Both assays demonstrated robust performance and broad linearity. Antibody titers were measured using fluorescent antibody to membrane antigen (FAMA) and ELISA. ADCP and ADCC activities, along with FAMA and ELISA geometric mean titers (GMTs), were significantly increased in post- versus pre-vaccination sera ($p < 0.0001$). Strong correlations were observed between ADCP and ADCC activities and both FAMA and ELISA GMTs. Although children exhibited lower total varicella-zoster virus-specific IgG levels than adults, higher IgG3 subclass levels in children were associated with comparable Fc-mediated activities. These results highlight the utility of ADCP and ADCC as valuable assays for evaluating Fc-mediated antibody function and as potential surrogates of protective immunity to varicella and zoster vaccination.

Varicella (chickenpox) and herpes zoster (HZ) are distinct clinical manifestations caused by the varicella-zoster virus (VZV), progressing from primary infection and viral reactivation, respectively. During primary infection, VZV spreads systemically through viremia, whereas HZ results from viral reactivation in sensory ganglia, followed by spread along peripheral nerves. These pathogenic differences imply distinct immune mechanisms for protection and disease control. Antibodies targeting VZV glycoproteins, which reflect neutralizing antibody activity, correlate strongly with protection against varicella[1]. By contrast, such antibodies do not prevent HZ, for which cellular immunity is critical[2,3]. Notably, children with isolated agammaglobulinemia are not prone to severe varicella[4]. However, VZV-specific memory T cell responses after vaccination remain weak or undetectable in children[5]. Severe or disseminated varicella has been reported in individuals with natural killer (NK) or invariant NKT-cell deficiencies, underscoring the importance of innate cellular immunity in controlling infection[6–9]. Together, these findings suggest that clearance of VZV-infected cells relies not only on T cells but also on cooperation between adaptive and innate immune responses.

Fc effector functions, such as antibody-dependent cellular phagocytosis (ADCP) and antibody-dependent cellular cytotoxicity (ADCC), enhance the clearance of virus-infected cells[10–17]. These functions may be particularly relevant for HZ, where the virus is presumed to evade neutralization[18]. Beyond Fab-mediated neutralization, antibodies exert their functions through the Fc domain, which recruits and activates innate immune cells, including macrophages and NK cells[19,20]. Fc-mediated effector functions have been implicated in protection against diverse viral infections, including herpes simplex virus-2 (HSV–2), dengue virus, respiratory syncytial virus (RSV), SARS-CoV-2, Ebola, and influenza[21–29]. Immunoglobulin G (IgG)

[1]Department of Microbiology, College of Medicine, Yeungnam University, Daegu, Republic of Korea. [2]BK21 Graduate Program, Department of Biomedical Sciences, College of Medicine, Korea University Guro Hospital, Seoul, Republic of Korea. [3]Department of Microbiology, College of Medicine, Ewha Womans University, Seoul, Republic of Korea. [4]Asia Pacific Influenza Institute, Korea University College of Medicine, Seoul, Republic of Korea. [5]Department of Convergence Medicine, College of Medicine, Korea University Guro Hospital, Seoul, Republic of Korea. [6]Division of Infectious Diseases, Department of Internal Medicine, Korea University College of Medicine, Seoul, Republic of Korea. [7]Immunogenicity Evaluation Laboratory, Clinical Trial Center, Yeungnam University Hospital, Daegu, Republic of Korea. ✉e-mail: hspark@ynu.ac.kr

utmb Health Sealy Institute for Vaccine Sciences

subclasses also differ in their ability to mediate Fc effector activity, with IgG3 generally exhibiting greater potency than IgG1[30]. Differential subclass responses have been reported in varicella and zoster infection[31], suggesting that host age and disease context may shape Fc-effector profiles.

Despite these insights, Fc-mediated antibody functions against VZV remain poorly characterized, and no standardized assays are currently available for their evaluation. This gap limits our understanding of protective immunity and hampers the development of reliable correlates of protection for VZV vaccines. To address this, we established physiologically relevant macrophage-based ADCP and NK cell-based ADCC assays and validated their reproducibility and robustness. Then, we applied these assays to sera from children and adults immunized with varicella and zoster vaccines, respectively. In parallel, antibody levels were measured by fluorescent antibody to membrane antigen (FAMA), ELISA, and IgG subclass analyses (Fig. 1). Together, these data provide the most comprehensive characterization to date of VZV-specific antibody functions across age groups and highlight their potential as functional biomarkers for evaluating vaccine-induced immunity.

Results

Establishment of ADCP and ADCC assay to assess varicella and zoster vaccine immunogenicity

We established an ADCP assay using carboxyfluorescein succinimidyl ester (CFSE)-labeled VZV-infected MRC-5 cells as target cells, employing M1-differentiated U937 cells as effector cells for evaluating human sera. To optimize the experimental conditions, U937 cells were differentiated into M1 macrophages using 20 ng/mL of each of PMA, LPS, and IFN-γ (Supplementary Fig. 1). The FcγRII (CD32) and FcγRI (CD64) were particularly upregulated in differentiated M1-U937 cells compared with U937 cells (Supplementary Fig. 2). These findings confirm that M1-U937 cells exhibit an activated macrophage phenotype. The ADCP activity was quantified as the percentage of $CFSE^{+}CD89^{+}$ double-positive cells by flow cytometry (Fig. 2a) and was further confirmed by confocal microscopy (Fig. 2b). Pre-vaccination sera did not induce detectable phagocytosis, as indicated by the absence of double-positive cells (Fig. 2b, left). In contrast, post-vaccination sera promoted robust phagocytosis of VZV-infected target cells by effector macrophages (Fig. 2b, right). For the ADCC assay, CMTMR-labeled VZV-infected MRC-5 cells served as target cells, employing the no-GFP-CD16.NK-92 cell line as an effector. Granzyme B (GrB)-uptake by target cells ($CMTMR^{+}GrB^{+}$ double-positive cells) was defined as the readout for ADCC detection (Fig. 2c). ADCC responses were also confirmed by confocal microscopy (Fig. 2d). Pre-vaccination sera induced negligible GrB uptake (Fig. 2d, left), but post-vaccination sera facilitated efficient transfer of GrB into target cells (Fig. 2d, right), confirming vaccine-induced Fc-mediated functional antibody responses.

Optimization of both assays involved assessing the effector-to-target (E:T) cell ratio, serum dilution, and the reaction time, using pre- and post-vaccination sera. E:T ratios of 1:2 and 2:1 (for ADCP) or 1:1 and 1:2 (for ADCC) were tested, followed by serial dilutions of sera at the optimal E:T ratios (1:2 for ADCP and 1:1 for ADCC). Incubation times of 2, 3, 4, or 5 hours were also evaluated. The final protocol of ADCP assay was established at an E:T ratio of 1:2, a 1:100 serum dilution, and a 4-hour incubation. The ADCC assay was conducted using an E:T ratio of 1:1, a 1:100 serum dilution, and a 4-hour incubation. (Supplementary Fig. 3, Supplementary Table 1).

Validation of ADCP and ADCC assays

Comprehensive validation of the ADCP and ADCC assays was performed using a VZV plasma panel together with pre- and post-VZV vaccination sera (Supplementary Table 2). Lot-to-lot variability of VZV-infected MRC-5 target cell stocks was assessed across three antibody concentrations. Given the cell-based nature of these assays, a coefficient of variation (CV) below 30% was predefined as an acceptance criterion. The range of target-cell lot-to-lot CVs was 1.0–5.8% for ADCP and 3.9–10.2% for ADCC, meeting this criterion (Fig. 3a, b; Supplementary Tables 3, 4). Linearity was evaluated using five serial dilutions of three samples. Simple linear regression analysis showed very strong linearity across a broad range (ADCP $r^2 = 0.87–0.96$; ADCC $r^2 = 0.87–0.97$) (Fig. 3c, d; Supplementary Tables 5, 6), supporting accurate quantification across varying antibody concentrations. Intra-assay precision was assessed by running five replicates of six panel samples on a single plate. For ADCP, intra-assay CVs were 5.7–29.2% (Fig. 3e, Supplementary Table 7) and ADCC intra-assay CVs were 3.0–27.9% across all six panels, meeting the acceptance criterion at low, medium, and high levels (Fig. 3f, Supplementary Table 8). Inter-assay precision was determined across three independent runs on different days by two operators. Between-operator CVs were 2.4–24.8% for ADCP (Fig. 3g, Supplementary Table 9) and 3.1–25.8% for ADCC (Fig. 3h, Supplementary Table 10). Inter-day CVs ranged from 4.2–19.8% for ADCP (Fig. 3i, Supplementary Table 11) and 0.1–29.3% for ADCC (Fig. 3j, Supplementary Table 12). Finally, inter-

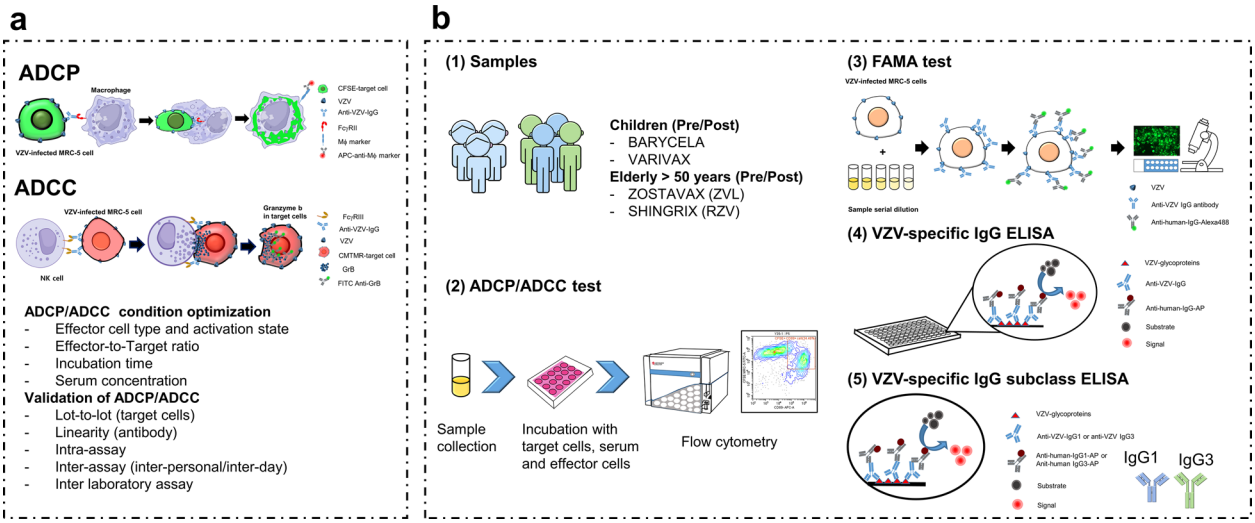


Fig. 1 | Study overview and workflow to quantify Fc-mediated effector functions and humoral immunity to VZV after varicella and zoster vaccination. **a** Schematic representation of ADCP and ADCC assays, highlighting key parameters for assay optimization and validation. **b** Application of ADCP and ADCC to samples from vaccinated children and adults, showing the workflow from sample collection to flow cytometric readout. Assessment of humoral immunity was performed using FAMA, VZV-specific IgG ELISA, and VZV-specific IgG subclass ELISA (IgG1, IgG3). LAV live attenuated varicella vaccine, RZV recombinant zoster vaccine, VZV varicella-zoster virus, ZVL live attenuated zoster vaccine.

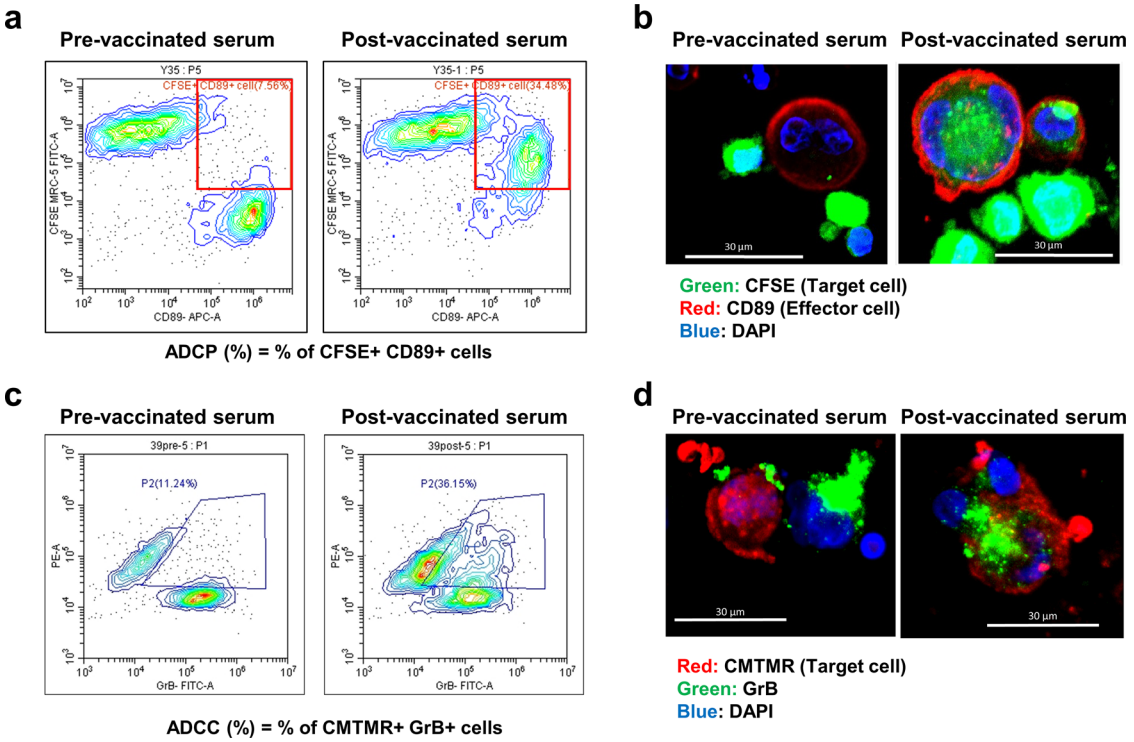


Fig. 2 | ADCP and ADCC activities measured by flow cytometry with representative confirmation by confocal microscopy. a Antibody-dependent cellular phagocytosis (ADCP) quantified by flow cytometry. VZV-infected MRC-5 target cells were labeled with CFSE and incubated with pre- (left panel) and post-varicella vaccination (right panel) sera, and then incubated with effector M1-U937 cells. M1-U937 cells were stained with APC-conjugated anti-CD89 antibody. ADCP activity was defined as the percentage of $CFSE^{+}CD89^{+}$ double-positive cells. **b** Confocal images of ADCP showing effector macrophages (red; anti-CD89-APC) containing CFSE-labeled VZV-infected MRC-5 target cells (green). No double-positive cells were detected with pre-varicella vaccination serum (left), whereas post-varicella vaccination serum induced efficient internalization of target cells into effector macrophages (right). Scale bar, 30 μm. **c** Antibody-dependent cellular cytotoxicity (ADCC) quantified by flow cytometry. VZV-infected MRC-5 target cells were labeled with CMTMR and incubated with pre- (left) and post-varicella vaccination (right) sera, and then incubated with effector NK cells. GrB was stained with FITC-conjugated anti-GrB antibody. ADCC activity was expressed as the percentage of $CMTMR^{+}GrB^{+}$ target cells. **d** Confocal images of CMTMR-labeled target cells (red) with internalized GrB (green) from effector cells. Pre-vaccination serum showed negligible GrB uptake (left), whereas post-vaccination serum promoted marked GrB internalization (right). Scale bar, 30 μm.

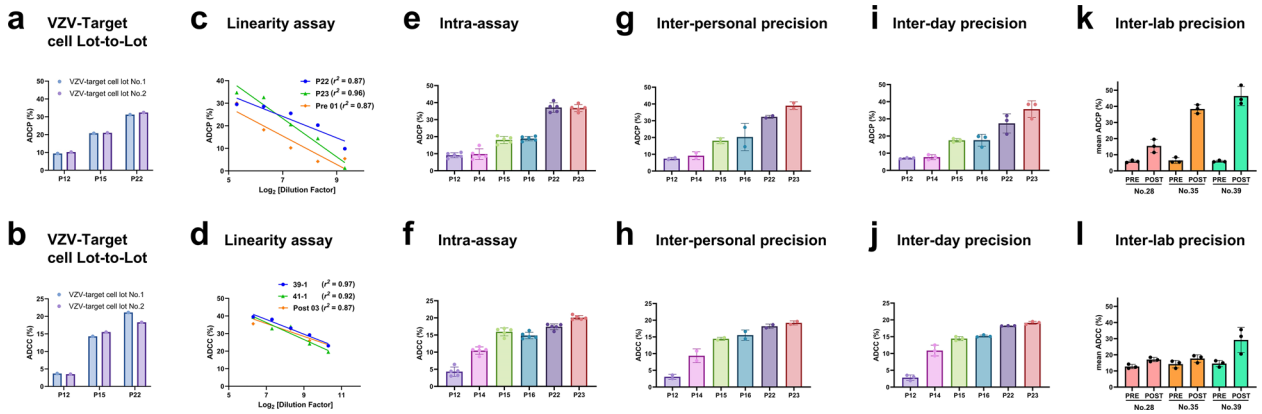


Fig. 3 | A series of validation experiments for the ADCP and ADCC assays. Lot-to-lot consistency: ADCP (**a**) and ADCC (**b**) activities were evaluated using two independent lots of VZV-infected MRC-5 target cell stocks, demonstrating consistent results across different target cell lots. Linearity: Five-point, two-fold serial dilutions of three representative sera were used to assess the linearity of the ADCP (**c**) and ADCC (**d**) responses, demonstrating strong proportionality between antibody dilution levels and Fc-mediated functional activities. Intra-assay precision: Repeatability of ADCP (**e**) and ADCC (**f**) assays was assessed by five replicate measurements of six samples in a single run, confirming assay reliability under identical conditions. Inter-operator (inter-personal) precision: ADCP (**g**) and ADCC (**h**) assays were performed independently by two operators across three separate runs to evaluate variability attributable to operator handling. Inter-day precision: Day-to-day reproducibility of ADCP (**i**) and ADCC (**j**) assays was assessed by repeated experiments over three separate days using the same set of samples. Inter-laboratory precision: ADCP (**k**) and ADCC (**l**) assays were conducted in three independent laboratories using paired pre- and post-vaccination sera to assess cross-site reproducibility.

laboratory testing across three laboratories using three paired pre-/post-vaccination sera showed comparable readouts, with inter-lab CVs of 7.0–26.6% for ADCP and 7.6–26.7% for ADCC (Fig. 3k, l; Supplementary Tables 13, 14). Together, these data indicate that the ADCP and ADCC assays using VZV-infected MRC-5 target cells are robust and reproducible across operators, days, and laboratories, and perform consistently across a broad range of antibody levels, supporting their utility for Fc-mediated antibody assessment in recipients of both varicella and zoster vaccines.

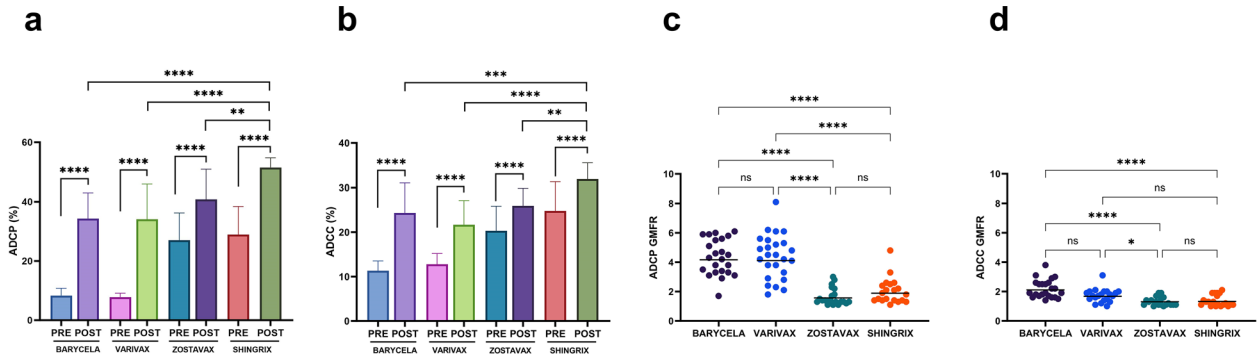


Fig. 4 | VZV-specific Fc-mediated responses following VZV immunization were measured by ADCP and ADCC assays. ADCP (**a**) and ADCC (**b**) activities measured in paired pre- and post-vaccination sera. GMFRs (post/pre) in ADCP (**c**) and ADCC (**d**) responses. Sera were collected from individuals who received one dose of BARYCELA (children, $n = 23$), one dose of VARIVAX (children, $n = 25$), one dose of ZOSTAVAX (adults, $n = 20$), or two doses of SHINGRIX (adults, $n = 20$). Statistical analyses were performed using a paired t-test, Wilcoxon matched-pairs signed-rank test, or the Kruskal−Wallis test with post hoc pairwise comparisons and appropriate corrections. Significance levels are indicated as $p < 0.05$ (*), $p < 0.01$ (**), $p < 0.001$ (***), $p < 0.0001$ (****), and ns (not significant). Data are presented as mean ± SD, with error bars indicating SD; GMFR, geometric mean fold rise.

Varicella or zoster vaccination induced ADCP and ADCC activities

Fc effector functions were evaluated using the ADCP and ADCC assays in pre- and post-vaccination sera from recipients of varicella or zoster vaccines. In the pre-vaccination sera of 1-year-old children receiving live attenuated varicella vaccines (LAVs), BARYCELA or VARIVAX, ADCP and ADCC activities were at baseline levels: BARYCELA (ADCP: 8.3%, ADCC: 11.3%) and VARIVAX (ADCP: 7.8%, ADCC: 12.8%). However, these activities significantly increased after a single dose of vaccination: BARYCELA (ADCP: 34.3%, ADCC: 24.3%) and VARIVAX (ADCP: 34.1%, ADCC: 21.7%) ($p < 0.0001$; Fig. 4a, b; Supplementary Table 15).

Since most Korean adults already possess immunity to VZV, pre-vaccination sera showed similar levels of ADCP and ADCC activities in the two zoster vaccine (ZV) groups, ZOSTAVAX (ADCP: 27.0%, ADCC: 20.3%) and SHINGRIX (ADCP: 28.9%, ADCC: 24.8%). Post-vaccination sera showed significant increases in ADCP and ADCC activities in ZOSTAVAX (ADCP: 40.8%, ADCC: 25.9%) after a single dose and SHINGRIX (ADCP: 51.5%, ADCC: 31.9%) after two doses, compared to pre-vaccination sera ($p < 0.0001$; Fig. 4a, b; Supplementary Table 15). A single dose of LAVs in children showed comparable ADCP and ADCC activities to a single dose of ZOSTAVAX in adults.

The geometric mean fold rises (GMFR) between pre- and post-vaccination were as follows BARYCELA: ADCP (4.2-fold), ADCC (2.1-fold), VARIVAX: ADCP (4.1-fold), ADCC (1.7-fold), ZOSTAVAX: ADCP (1.6-fold), ADCC (1.3-fold), and SHINGRIX: ADCP (1.9-fold), ADCC (1.3-fold). Therefore, there were no significant differences in fold changes between BARYCELA and VARIVAX or between ZOSTAVAX and SHINGRIX recipients (Fig. 4c, d; Supplementary Table 15).

Antibody titers measured by the FAMA test and ELISA

Antibody titers were measured by the FAMA test, the gold standard method for the varicella vaccine-induced antibody titer, and ELISA. The geometric mean titers (GMTs) of FAMA in post-vaccination sera for all four vaccine groups were significantly higher than those in pre-vaccination sera ($p < 0.0001$) (Fig. 5a). GMTs of pre-vaccinated children's sera (BARYCELA and VARIVAX) were negative levels (≤2.2). Post-BARYCELA GMT (153.4: ranging from 32 to 512) and post-VARIVAX GMT (164.3: range, 32–1024) were significantly increased, but there were no differences between two vaccines. The FAMA GMTs of pre-vaccinated adults' sera showed similar levels; pre-ZOSTAVAX (78.8: range, 32–256) and pre-SHINGRIX (87.4: range, 32–256). However, those of post-SHINGRIX (776.0: range, 256–2048) were significantly higher than post-ZOSTAVAX (215.3: range, 64–512) (Fig. 5a, Supplementary Table 16).

Anti-VZV IgG ELISA antibody titers were measured using VZV IgG Serion ELISA classic kit (detection range, 15–2000 mIU/mL). The GMTs of anti-VZV IgG ELISA antibodies in the post-vaccinated sera were significantly elevated relative to pre-vaccination levels in all groups ($p < 0.0001$; Fig. 5b). Most pre-vaccinated children's sera were lower than the detection limit; pre-BARYCELA GMT (0.8 mIU/mL: range, 0.1–32.0 mIU/mL) and pre-VARIVAX GMT (0.4 mIU/mL: range, 0.01–24.8 mIU/mL). Post-BARYCELA GMT (118.9 mIU/mL: range, 27.8–435.4 mIU/mL) and post-VARIVAX GMT (139.2 mIU/mL: range, 37.5–893.2 mIU/mL) were significantly increased, but there were no differences between the two vaccines (Fig. 5b, Supplementary Table 17). The ELISA GMTs of pre-vaccinated adults' sera showed similar levels, pre-ZOSTAVAX GMT (520.1 mIU/mL: range, 159.1–1484.4 mIU/mL) and pre-SHINGRIX GMT (609.6 mIU/mL: range, 145.0–2176.0 mIU/mL). However, all of the post-SHINGRIX samples, the ELISA titers were over the detection limit; post-SHINGRIX GMT (10,428.9 mIU/mL: range, 4561.4–36,355.9 mIU/mL) and significantly higher than post-ZOSTAVAX GMT (1697.3 mIU/mL: range, 415.2–4599.2 mIU/mL) (Fig. 5b, Supplementary Table 17).

Differential expression of anti-VZV IgG1 and IgG3 in varicella-vaccinated children and zoster-vaccinated adults

To characterize subclass-specific antibody responses induced by VZV vaccination, IgG1 and IgG3, key mediators of ADCP and ADCC responses, were quantified by ELISA. Distinct IgG subclass profiles were observed between varicella-vaccinated children and zoster-vaccinated adults. Both IgG1 and IgG3 antibody levels significantly increased after vaccination in all groups ($p < 0.0001$, Fig. 5c, d). Analysis of IgG1 subclass GMFRs revealed that children who received LAVs exhibited significantly lower increases: BARYCELA (1.6) and VARIVAX (2.0), compared with adults vaccinated with HZ vaccines, ZOSTAVAX (3.7) and SHINGRIX (7.3) (Fig. 5e, Supplementary Table 18). Conversely, IgG3 subclass GMFRs were significantly higher in children immunized with LAVs −BARYCELA (4.4) and VARIVAX (5.5), than in adults vaccinated with ZOSTAVAX (1.4) or SHINGRIX (1.6) (Fig. 5f, Supplementary Table 18). These findings indicate that first exposure to varicella vaccination in children preferentially induces IgG3 responses, whereas adult zoster vaccination elicits a predominant IgG1 response.

In children, both IgG1 and IgG3 levels showed significant correlations with ADCP, ADCC, FAMA titer, and ELISA titer. However, IgG3 exhibited stronger correlations with ADCP, ADCC, and FAMA titer compared to IgG1 (Fig. 6a−h). Correlation coefficients (r) between IgG1 and ADCP, ADCC, and FAMA were 0.563 ($p < 0.0001$), 0.340 ($p < 0.0012$), and 0.545 ($p < 0.0001$), respectively (Fig. 6a−c). Whereas those between IgG3 and the same parameters were higher, 0.804, 0.647,

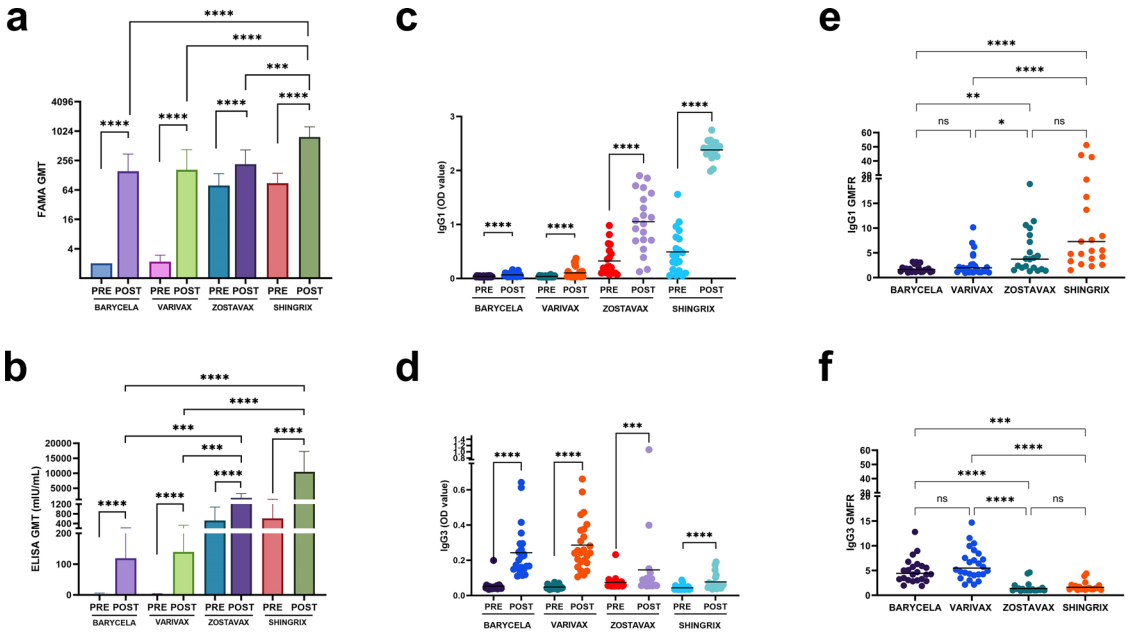


Fig. 5 | VZV-specific humoral immune responses before and after vaccination. Paired pre- and post-vaccination sera were analyzed from individuals who received one dose of BARYCELA (children, $n = 23$), one dose of VARIVAX (children, $n = 25$), one dose of ZOSTAVAX (adults, $n = 20$), or two doses of SHINGRIX (adults, $n = 20$). **a** FAMA geometric mean titers (GMTs). **b** VZV-specific IgG antibody titers quantified using the Serion ELISA Classic VZV IgG kit. VZV-specific IgG1 (**c**) and IgG3 (**d**) subclass levels measured by ELISA. GMFR comparisons of IgG1 (**e**) and IgG3 (**f**) responses in the four vaccine groups. Each dot represents an individual participant; lines indicate medians. Statistical analyses were performed using paired t-tests, Wilcoxon matched-pairs signed-rank tests, or the Kruskal–Wallis test with post hoc pairwise comparisons with appropriate corrections. Significance levels are indicated as $p < 0.05$ (*), $p < 0.01$ (**), $p < 0.001$ (***), $p < 0.0001$ (****), and ns (not significant). Data are presented as mean ± SD, with error bars indicating SD; GMFR, geometric mean fold rise.

and 0.802, respectively (all with $p < 0.0001$, Fig. 6e–g). However, the correlations between ELISA titers and IgG1 ($r = 0.775$) or IgG3 ($r = 0.744$) were comparable (Fig. 6d, h). In contrast, among zoster-vaccinated adults, strong and significant correlations were found between IgG1 and ADCP ($r = 0.856$), ADCC ($r = 0.698$), FAMA titer ($r = 0.939$), and ELISA titer ($r = 0.791$), all with $p < 0.0001$ (Fig. 6i–l). However, the correlations between IgG3 and these parameters were weak and not significant ($p > 0.05$, Fig. 6m–p). These findings suggest that IgG3 may play a more prominent role in vaccine-induced Fc-mediated antiviral functions in children, whereas IgG1 appears to be more critical in adults.

Correlation between Fc-mediated antibody functions (ADCP, ADCC) and antibody titers (FAMA, ELISA) across vaccine types

Pearson correlation analysis was performed to determine the relationships between Fc-mediated antibody functions (ADCP and ADCC) and antibody titers (FAMA and ELISA) across different vaccine types. Robust and statistically significant correlations were observed between ADCP activity and FAMA titers across all vaccine groups: BARYCELA ($r = 0.947$), VARIVAX ($r = 0.936$), ZOSTAVAX ($r = 0.809$), and SHINGRIX ($r = 0.885$) (Fig. 7a–d; all $p < 0.0001$), indicating a very strong correlation between these two immunological parameters. Similarly, ADCC activities were strongly correlated with FAMA titers in all vaccine groups: BARYCELA ($r = 0.837$), VARIVAX ($r = 0.705$), ZOSTAVAX ($r = 0.707$), and SHINGRIX ($r = 0.630$) (Fig. 7e–h, all $p < 0.0001$).

In contrast, correlations of ADCP and ADCC with ELISA titers were relatively weaker than those with FAMA titers, though still statistically significant. For ADCP, the correlations with ELISA were: BARYCELA ($r = 0.890$), VARIVAX ($r = 0.761$), ZOSTAVAX ($r = 0.853$, $p < 0.001$), and SHINGRIX ($r = 0.702$) (Fig. 7i–l, all other $p < 0.0001$). For ADCC, the correlations with ELISA were: BARYCELA ($r = 0.823$), VARIVAX ($r = 0.500$), ZOSTAVAX ($r = 0.667$), and SHINGRIX ($r = 0.567$) (Fig. 7m–p, all $p < 0.0001$). Moderate to very strong correlations were also noted between ADCC and ADCP within each vaccine group; BARYCELA ($r = 0.854$), VARIVAX ($r = 0.632$), ZOSTAVAX ($r = 0.655$), and SHINGRIX ($r = 0.748$) (Fig. 7q–t, all $p < 0.0001$).

In the overall VZV-vaccinated population, ADCP and ADCC activities were strongly correlated with each other ($r = 0.806$, $p < 0.0001$) and with FAMA titers (ADCP: $r = 0.917$; ADCC: $r = 0.806$; both $p < 0.0001$) (Fig. 8a–c). In comparison, their correlations with ELISA titers were moderate (ADCP: $r = 0.529$; ADCC: $r = 0.505$; both $p < 0.0001$) (Fig. 8d, e).

These findings demonstrate that ADCP and ADCC show stronger correlations with FAMA titers than with gpELISA titers. Given that FAMA titers represent a well-established correlate of protection (CoP) against varicella and a sensitive surrogate of neutralizing antibody responses for varicella vaccines, these findings suggest that Fc-mediated functional assays capture not only the capacity to eliminate VZV-infected cells, but also immunological information closely aligned with neutralizing antibody activity.

Discussion

Varicella is a highly contagious infectious disease, and live attenuated varicella vaccines have been incorporated into national immunization programs in many developed countries[32]. Meanwhile, global demand for varicella vaccines continues to grow, highlighting the importance of accurate immunogenicity assessment. In addition, HZ remains a significant global health concern, with increasing incidence and limited vaccine availability[33]. Varicella-zoster virus (VZV) infection and reactivation are controlled by multiple, non-redundant immune mechanisms, and each immunological readout captures a distinct layer of vaccine-induced protection. During primary varicella infection, viral dissemination occurs through both cell-free viral particles and T-cell–associated viremia, in which infected T cells traffic virus to the skin[34]. Consequently, neutralizing antibodies may not completely block hematogenous spread but can limit extracellular virus and reduce overall viral burden. In this context, observations that patients with agammaglobulinemia do not progress to severe varicella[4] and that

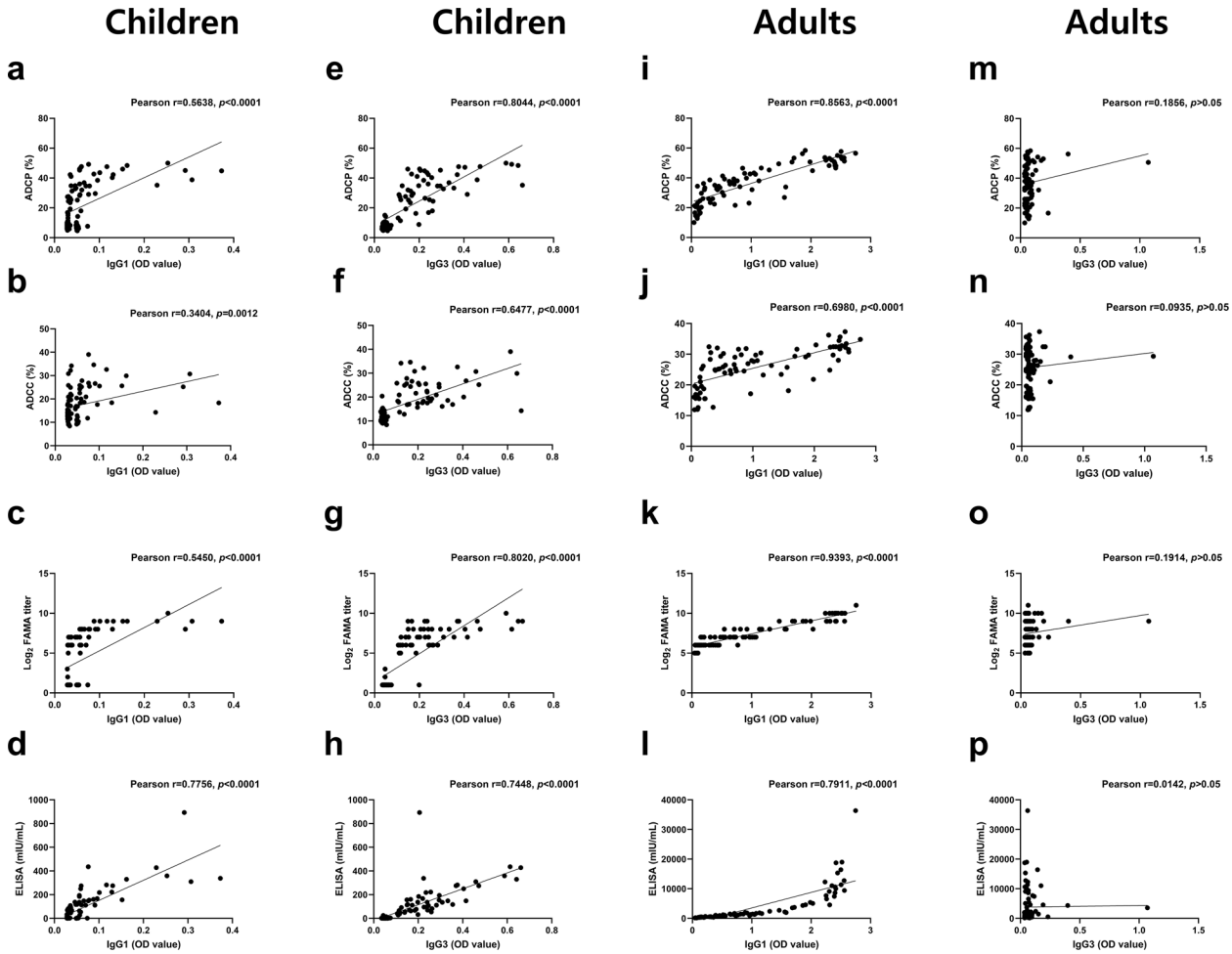


Fig. 6 | Correlation of ADCP, ADCC, FAMA, and ELISA titers with VZV-specific IgG1 and IgG3 subclass levels in vaccinated individuals. Correlation analyses were performed using pre- and post-vaccination sera from children who received varicella vaccines (BARYCELA and VARIVAX) and adults who received zoster vaccines (ZOSTAVAX and SHINGRIX). **a**–**d** Correlations between IgG1 levels and ADCP, ADCC, FAMA titers, and ELISA titers in children. **e**–**h** Correlations between IgG3 levels and the same parameters in children. **i**–**l** Correlations between IgG1 levels and ADCP, ADCC, FAMA titers, and ELISA titers in adults. **m**–**p** Correlations between IgG3 levels and the same parameters in adults. Pearson's correlation coefficients (r) and corresponding p values are shown in each panel.

children exhibit minimal VZV-specific T-cell responses[5,35] suggest that innate cellular immunity plays a critical role in protection. Clearance of virus-infected cells, however, requires cell-mediated effector mechanisms. While cytotoxic T lymphocytes play a central role in eliminating intracellular virus, T-cell immunity is relatively immature in young children following primary varicella vaccination. Under these conditions, Fc-mediated antibody functions that bridge humoral immunity with innate effector cells become particularly important. Antibody-dependent cellular cytotoxicity (ADCC) and antibody-dependent cellular phagocytosis (ADCP), mediated by natural killer cells and macrophages, may therefore contribute substantially to the elimination of VZV-infected cells and to disease resolution in pediatric populations. Therefore, it is important to evaluate the contribution of Fc-mediated antibody functions in cooperation with innate immune effector cells when assessing the protective efficacy of varicella vaccines.

HZ, caused by the reactivation of dormant VZV in the ganglia and its spread via nerve fibers, cannot be prevented solely by neutralizing antibodies. Instead, cellular immune responses play a critical role in protection. Therefore, HZ vaccine-induced immunity has been assessed not only by antibody titers but also through T-cell readouts, including cytokine secretion (e.g., IFN-γ, IL-2, and TNF-α) in PBMCs and the frequency of polyfunctional $CD4^+$ and $CD8^+$ T cells[36–40]. However, compared with other herpesviruses such as cytomegalovirus or herpes simplex virus type 1, VZV is characterized by a relatively low frequency of circulating memory T cells, even in adults[41]. This limitation underscores that current cellular immune readouts may not fully reflect the clearance of virus-infected cells, and contributes to the absence of a definitive CoP for HZ vaccines, necessitating large-scale clinical follow-up studies to assess their efficacy.

In this context, Fc-mediated antibody functions may represent an important complementary mechanism of antiviral defense that interfaces between humoral immunity and innate cellular responses. ADCP and ADCC capture immune mechanisms not fully reflected by either neutralizing antibody or T-cell-based assays alone and may therefore provide mechanistically relevant insights into virus clearance. Supporting this concept, Fc-mediated effector functions have been associated with improved viral control or protection in multiple viral infections, including HIV and SARS-CoV-2, and impaired ADCC and ADCP responses have been linked to severe disease outcomes in humans and animal models[42–47]. In a previous study on varicella, ADCC activity was detected earlier than neutralizing antibody responses following natural infection or live attenuated vaccine, suggesting a key role for Fc-mediated functions during the early phase of VZV infection[48]. While ADCC induction by zoster vaccination has been speculated[18], the capacity of the zoster vaccines to elicit ADCP and ADCC has not been comprehensively evaluated using physiologically relevant systems.

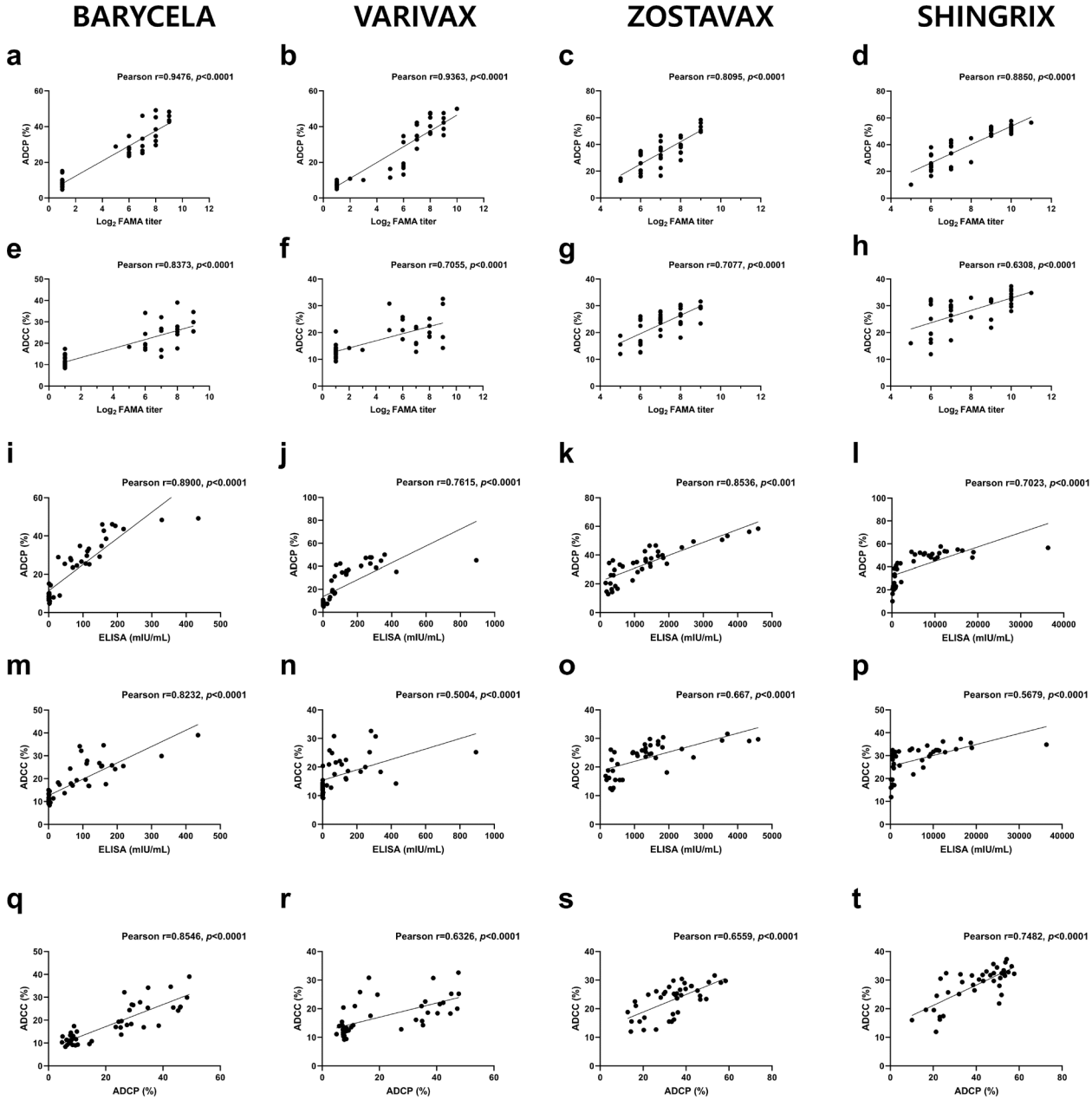


Fig. 7 | Correlation of ADCP and ADCC activities with FAMA titers, ELISA antibody titers, and between each other, stratified by vaccine type. Scatter plots show the correlations between FAMA titers and ADCP (**a**–**d**) or ADCC (**e**–**h**), between ELISA antibody titers and ADCP (**i**–**l**) or ADCC (**m**–**p**), and between ADCP and ADCC (**q**–**t**) in recipients of BARYCELA (**a**, **e**, **i**, **m**, **q**), VARIVAX (**b**, **f**, **j**, **n**, **r**), ZOSTAVAX (**c**, **g**, **k**, **o**, **s**), and SHINGRIX (**d**, **h**, **l**, **p**, **t**). Each dot represents an individual recipient. Pearson correlation coefficients (r) and corresponding p values are indicated in each panel. Positive, statistically significant correlations were observed across all vaccine types.

To address this gap, we developed physiologically relevant ADCP and ADCC assays using VZV-infected MRC-5 cells as target cells, employing macrophages as effector cells for ADCP and NK cells for ADCC. This design better reflects the complex antigenic profile of live attenuated VZV vaccines (e.g, BARYCELA, VARIVAX, and ZOSTAVAX), which elicit antibodies against multiple VZV antigens, thereby providing a broader assessment of antibody functionality than gE-transfected systems.

Both ADCP and ADCC assays demonstrated high reproducibility and robustness. Importantly, their activities correlated strongly with FAMA titers, supporting their validity as functional surrogate markers for protective immunity to varicella. While FAMA primarily reflects the presence of neutralizing antibodies, ADCP and ADCC capture mechanistically distinct aspects of antiviral immunity by integrating antibody quality with the capacity to recruit innate effector cells. Our key finding is that all tested VZV vaccines elicited antibodies capable of mediating ADCP and ADCC against VZV-infected target cells across vaccine platforms and age groups relevant to their real-world, clinically approved use.

Interestingly, although the ELISA-based antibody concentrations were significantly higher in adults vaccinated with zoster vaccines than in children who received LAVs, Fc-mediated functions (ADCP and ADCC) were comparable across the live attenuated vaccine platforms regardless of age. This indicates that children generate antibodies with enhanced Fc-effector functionality despite lower total IgG levels. IgG subclass analysis revealed higher IgG3 and lower IgG1 levels in children than in adults. This is consistent with previous observations that varicella vaccination or primary varicella infection in children elicits an IgG3-dominant response, whereas adults with HZ exhibit an IgG1-dominant profile[31,49]. Age-related shifts in IgG subclasses align with reports from other viral infections, including RSV

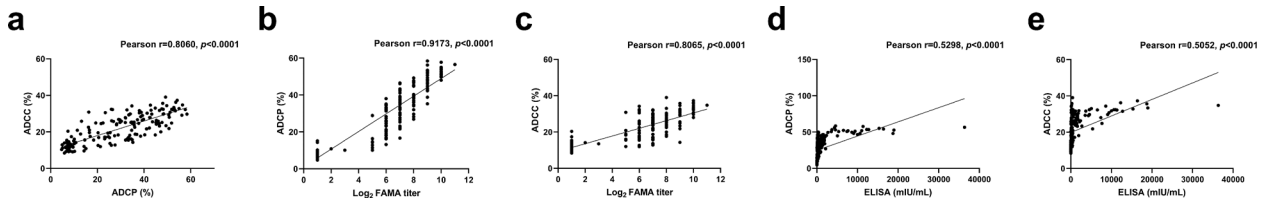
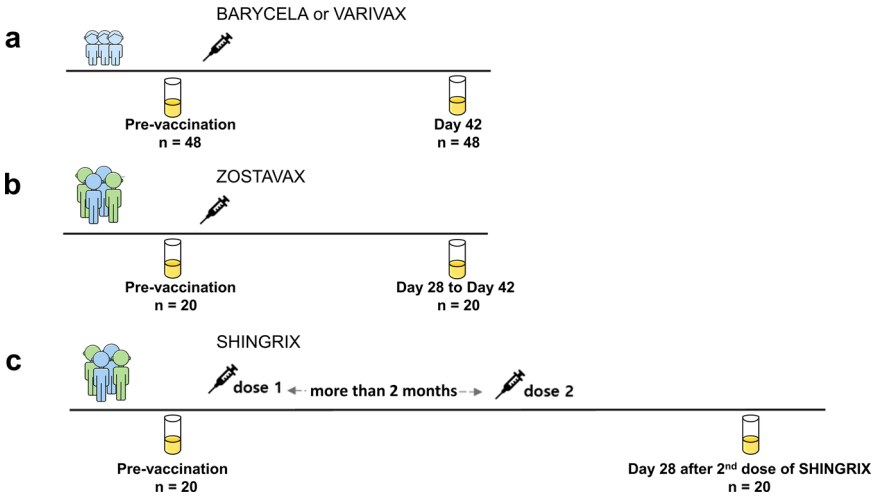


Fig. 8 | Correlations among ADCP, ADCC, FAMA titers and ELISA antibody titers across all vaccine groups. Scatter plots show correlations between ADCP and ADCC (**a**), FAMA titers and ADCP (**b**) or ADCC (**c**), and ELISA antibody titers and ADCP (**d**) or ADCC (**e**) using pooled data from all vaccine recipients. Each dot represents an individual serum sample. Pearson correlation coefficients (r) and corresponding p values are indicated in each panel.

Fig. 9 | Study design for vaccination and sample collection schedules. a Healthy children were vaccinated with either BARYCELA ($n = 23$) or VARIVAX ($n = 25$); sera were collected at baseline and on Day 42 post-vaccination. **b** Healthy adults ($n = 20$) received a single dose of ZOSTAVAX; sera were collected at baseline and between Days 28 and 42 post-vaccination. **c** Healthy adults ($n = 20$) received two doses of SHINGRIX administered ≥ 2 months apart; sera were collected at baseline and 28 days after the second dose.



and measles, where IgG3 predominates in young children but declines with age[50]. The subclass-specific differences observed here reflect known distinctions in Fc receptor engagement on effector cells and the biological activities of IgG subclasses[51]. In the RV144 vaccine trial, depletion of IgG3 antibodies significantly reduced ADCP and ADCC activities, underscoring the importance of IgG3 in Fc-effector function[52]. Together, these data illustrate how qualitative features of the humoral response, such as IgG subclass composition, shape functional interactions with innate immune cells and contribute to effective antiviral immunity across age groups.

The sample size was insufficient to assess the impact of demographic characteristics beyond sex-based differences, such as age-dependent or population-level variability. However, the sample size was sufficient for the primary objectives of this study, which were the development and validation of the ADCP and ADCC assays and the evaluation of their analytical robustness and feasibility across different VZV vaccine platforms and clinically relevant target populations. Second, we employed M1-differentiated U937 cells or the No-GFP-CD16.NK-92 cell line as effector cells rather than autologous innate immune cells from vaccinees. As a result, we were unable to assess ADCP and ADCC activities mediated by the vaccinees' own effector cells. Nevertheless, the use of standardized effector cell lines helps to minimize inter-individual variability, which is crucial for evaluating vaccine-induced antibody functions in clinical trials.

We developed cell-based ADCP and ADCC assays that provide physiologically relevant measures of Fc-mediated antibody function against VZV. These assays correlated more strongly with FAMA titers than with ELISA antibody levels. Children, despite lower overall IgG levels, mounted potent IgG3-driven ADCP and ADCC activities comparable to adults. By integrating humoral antibody levels, Fc-mediated effector functions, and innate cellular engagement, these findings highlight the importance of antibody quality over quantity and suggest that incorporating ADCP and ADCC assays alongside conventional serological tests may provide a more comprehensive, mechanistic assessment of VZV vaccine-induced immunity.

Methods

Ethics statement and Sera from vaccinees

Human specimens were obtained from pediatric LAV recipients enrolled in the Phase 3 clinical trial of MG1111 (Thailand and South Korea, protocol No. NCT03375502) and from adult ZOSTAVAX recipients (IRB file No. YUH-12-0462) conducted in Yeungnam University Medical Center. Written informed consent for secondary research use of banked specimens was obtained from all participants or their legal guardians. Secondary use for this study was approved by the Institutional Review Board of Yeungnam University Medical Center (IRB No. YUMC 2023-04-034). Blood collection from SHINGRIX recipients was approved by the Institutional Review Board of Korea University Guro Hospital (IRB No. 2023GR0083). All samples were de-identified prior to transfer. The study was conducted in accordance with the Declaration of Helsinki, ICH E6(R2) Good Clinical Practice guidelines, as well as applicable local regulatory and bioethics requirements.

Paired pre- and post-vaccination plasma/serum samples were obtained from four cohorts representing the standard, clinically approved target populations of licensed VZV vaccines: 1-year-old children who received a single dose of LAV (BARYCELA® [GC Biopharma] or VARIVAX® [Marck & Co.]) and adults aged ≥ 50 years old who received ZOSTAVAX® (Merck & Co.) or SHINGRIX® (GlaxoSmithKline). In total, 176 samples were analyzed: 46 from the BARYCELA® group, 50 from the VARIVAX® group, and 40 samples each from the ZOSTAVAX® and SHINGRIX® groups (Fig. 9).

Cells

MRC-5 cells (ECACC, UK) were cultured in Minimal Essential Medium (MEM; Welgene Inc.) supplemented with 10% fetal bovine serum (FBS; Gibco), 1% non-essential amino acid (NEAA; Sigma-Aldrich), 1% sodium pyruvate (Gibco), and 1× antibiotic-antimycotic (antibiotic; Gibco) at 37 °C in 5% CO_2. U937 cells (ATCC®; CRL-1593.2) were maintained in Roswell Park Memorial Institute (RPMI) 1640 medium (SERANA) supplemented with 10% heat-inactivated FBS (HI-FBS; Gibco) and antibiotics. No-GFP-CD16.NK-92 cell line (ATCC®; PTA-6967) was cultured in α-Minimum

Essential Medium (α-MEM; Gibco) supplemented with 12.5% HI-FBS, 12.5% horse Serum (Sigma-Aldrich), 0.2 mM myo-inositol (Sigma-Aldrich), 0.02 mM folic acid (Sigma-Aldrich), 1× antibiotic, 0.1 mM 2-mercaptoethanol (Gibco), and 100 U/mL IL-2 (R&D Systems).

Differentiation of U937 cells into M1 macrophages

To generate M1-polarized macrophages from U937 monocytes, 2×10^6 U937 cells in 5 mL of complete culture medium were treated with 20 ng/mL of phorbol 12-myristate 13-acetate (PMA; Sigma-Aldrich) for 24 h at 37 °C in 5% CO_2. After PMA treatment, non-adherent cells were removed, and the culture was washed twice with Dulbecco's phosphate-buffered saline (DPBS; SERANA) and then incubated for an additional 24 h in fresh medium. To induce M1 polarization, cells were stimulated with 20 ng/mL of lipopolysaccharide (LPS; Sigma-Aldrich) and 20 ng/mL of interferon-gamma (IFN-γ; R&D Systems) for 24 h before the ADCP assay. Morphological changes were monitored by light microscopy (Carl Zeiss) (Supplementary Fig. 1).

Flow cytometric analysis of Fcγ receptors

M1-polarized U937 cells were stained separately with fluorochrome-conjugated antibodies against CD16, CD32, and CD64 (BioLegend; Table 1) in 2% FBS-DPBS for 30 min on ice. Cells were then washed twice with 2% FBS-DPBS before acquisition on the CytoFLEX flow cytometer (Beckman Coulter).

VZV-infected target cell preparation

VZV-infected cells were prepared as target cells as described follows: MRC-5 cells at 70%–80% confluence were infected with VZV YC03 strain (GenBank Accession No. KJ808816) at a ratio of 1 infected cell to 100 normal MRC-5 cells. The cells were harvested 72 h post-infection and cryopreserved in liquid nitrogen until use. The percentage of cells expressing VZV antigens on the cell surface was determined using a flow cytometry-based FAMA test[53]. The WHO International standard for VZV immunoglobulin (NIBSC code W1044, diluted to 50 mIU/mL) was used as a positive reference, and DPBS served as the negative control. Following FAMA staining, VZV antigen-expressing cells were analyzed using the CytoFLEX flow cytometer (Beckman Coulter). Cell preparations exhibiting ≥ 80% VZV-positive events were used as target cells in ADCP and ADCC assays.

Antibody-dependent cellular phagocytosis assay

The phagocytic activity was evaluated using M1-differentated U937 as effector cells. Sera were heat-inactivated for 30 min at 56 °C before the assay. VZV-infected MRC-5 target cells were labeled with 3 μM CFSE [5-(and-6)-Carboxyfluorescein Diacetate, Succinimidyl Ester] in DPBS for 10 min at 37 °C and then washed twice with DPBS supplemented with 2% HI-FBS. The CFSE-labeled target cells were incubated with control or vaccinated sera for 30 min and then co-incubated with M1-U937 effector cells at an effector cell-to-target (E:T) ratio of 1:2 for 4 h. Sera were applied at final dilution of 1:100. During initial assay validation, mock-infected (uninfected) MRC-5 target cells were included to confirm antigen non-specific ADCP activity (Supplementary Fig. 4a). Prior to flow cytometry, M1-U937 cells were labeled with CD89 antibody conjugated to APC (Miltenyi Biotec), which was used solely as a cell surface marker to discriminate effector cells from CFSE-labeled target cells for gating purposes. ADCP activity, measured using the CytoFLEX flow cytometer (Beckman Coulter), was expressed as the percentage of $CFSE^+CD89^+$ double-positive macrophages that phagocytosed $CFSE^+$ VZV-infected cells.

Table 1 | Antibodies used for flow cytometric analysis of Fcγ receptors

Target	Full name	Clone	Fluorochrome	Catalog No. (BD)
CD16	FcγRIII	3G8	FITC	560996
CD32	FcγRII	FLI8.26	PE	568913
CD64	FcγRI	10.1	APC	561189

Antibody-dependent cellular cytotoxicity assay: measuring granzyme B (GrB+) incorporation into target cells by flow cytometry

To measure ADCC activities, an assay measuring GrB^+ incorporation into VZV-infected MRC-5 target cells was adopted from the ADCC-GTL assay[54]. VZV-infected target cells were labeled with 5 μM CellTracker™ Orange CMTMR (5-(and-6)-((((4-chloromethyl)benzoyl) amino) tetramethylrhodamine; Invitrogen) in serum-free AIM-V medium (Gibco) for 30 min at 37 °C. Labeled cells were washed once with serum-free AIM-V medium, and 2×10^4 cells per well were plated in 96-well U-bottom plates. Heat-inactivated sera were added and incubated with target cells for 30 min at 37 °C. No-GFP-CD16.NK-92® cells were then added at a 1:1 E:T ratio, yielding a final serum dilution of 1:100. Co-cultures were incubated for 4 h at 37 °C before harvest. Cells were fixed with 100 μL/well of Fixation/Permeabilization solution (BD Biosciences) for 20 min at 4 °C, washed twice with 1× BD Perm/Wash™ buffer (BD Biosciences), and pelleted. The fixed/permeabilized cells were resuspended thoroughly in 100 μL of 1× BD Perm/Wash™ buffer containing FITC-conjugated anti-Granzyme B (GrB) antibody at a 1:50 dilution (BioLegend). The samples were incubated for 30 min at 4 °C in the dark. After incubation, cells were washed twice with 1× BD Perm/Wash™ buffer and resuspended in 1× BD Perm/Wash™ buffer for flow cytometric analysis. ADCC activities, measured using the CytoFLEX flow cytometer (Beckman Coulter), was expressed as the percentage of $CMTMR^+$ GrB^+ double-positive target cells. During initial assay validation, mock-infected (uninfected) MRC-5 target cells were included to verify antigen non-specific ADCC responses (Supplementary Fig. 4b).

Validation of ADCP and ADCC assays

Following established bioanalytical assay validation guidelines[55,56], key performance parameters were selected for methodological evaluation of ADCP and ADCC assays. These parameters included VZV-target cell lot-to-lot variation, linearity, intra-assay precision, inter-assay precision (inter-personal and inter-day precision), and inter-laboratory precision.

Lot-to-lot variability was evaluated to determine the consistency of assay results across different target cell stocks used in the same experiment, ensuring that variations between target cells do not significantly affect assay outcomes. Linearity was assessed using five serial dilutions of each of three different sera, with a simple linear regression analysis performed to confirm linearity. Intra-assay precision was assessed by testing six samples, each tested in five replicates on the same plate by one operator, to determine the assay's precision within a single run. Inter-assay precision was assessed by testing the same six samples across three days by two different operators, to assess reproducibility across independent experiments. Inter-laboratory precision was determined by having three laboratories independently conduct the assay using identical sera and the same stock of VZV-target cells, ensuring reproducibility across different laboratory settings. The coefficient of variation (CV) was calculated to assess assay precision. Given the cell-based nature of the ADCP and ADCC assays, which involve effector cells, live virus-infected target cells, and antibodies, these assays inherently exhibit greater variability than cell-free biochemical assays. Therefore, a CV ≤30% was predefined as an acceptance criterion for assay precision, in accordance with commonly applied thresholds for cell-based functional assays[57–59].

Fluorescent antibody to membrane antigen test

The FAMA test was conducted as previously described[60]. Briefly, FAMA antigens were prepared as follows: MRC-5 cells at 70%–80% confluence were infected with the VZV YC03 strain at a ratio of one infected cell to 200 normal MRC-5 cells and harvested 72 h post-infection, and stored in liquid nitrogen until use. Sera were twofold serially diluted in DPBS, and then incubated with 2×10^5 FAMA antigen cells for 30 min at RT, followed by two DPBS washes. After incubation with the secondary antibody (goat anti-human IgG-Alexa Fluor 488; Invitrogen) for 30 min at RT, cells were

washed three times with DPBS. FAMA antigen cells were loaded onto a 14-well glass slide (Cel-Line®, Thermo Scientific) and then dried. Slides were mounted with Vectashield mounting medium with DAPI (Vector Laboratories) and observed using an Axioscope fluorescence microscope equipped with an HBO 100 mercury lamp (Carl Zeiss).

VZV-specific IgG ELISA

VZV-specific IgG levels were quantified using the SERION ELISA classic kit (ESR104G, Virion\Serion, Germany) according to the manufacturer's instructions. Briefly, 100 µL of controls and diluted sera were added to VZV-antigen-coated wells and incubated for 1 h. After washing, 100 µL of goat anti-human IgG conjugated to alkaline phosphatase (AP) was added and incubated for 30 min. Following additional washes, substrate was added and incubated for 30 min. All incubation steps were performed at 37 °C. The reaction was then terminated with a stopping solution, and the absorbance was measured at 405 nm using a Multiskan FC 357 microplate photometer (Thermo Scientific).

VZV-specific IgG subclass ELISA

VZV-specific IgG1 and IgG3 antibodies were measured using the SERION ELISA classic kit (ESR104G, Virion\Serion) with modifications. VZV antigen-coated plates were incubated with 100 µL of diluted sera (1:50) for 1 h at 37 °C. After washing, plates were incubated with mouse anti-human IgG1 (1:2000) or IgG3 (1:100) antibodies conjugated to AP (SouthernBiotech) at 37 °C for 30 min. Following incubation with pNPP substrate for 30 min, the reaction was stopped, and absorbance was measured at 405 nm using a Multiskan FC 357 microplate Photometer (Thermo Scientific). Subclass-specific responses were expressed as optical densities.

Statistical analyses

Statistical analyses were performed using GraphPad Prism 10.0.2 (GraphPad Software). Paired t-tests or Wilcoxon matched-pairs signed-rank tests were used for comparisons between two groups. One-way ANOVA or the Kruskal–Wallis tests were used for multiple group comparisons, with post-hoc pairwise correction as appropriate. Pearson correlation coefficients (r) were calculated to assess relationships among ADCP, ADCC, FAMA, and ELISA GMTs. Statistical significance was denoted as ns, not significant; * $p < 0.05$; ** $p < 0.01$; *** $p < 0.001$; **** $p < 0.0001$.

Data availability

The data supporting the findings of this study are available from the corresponding author upon reasonable request. This study did not generate or analyze datasets that require deposition in a public repository.

Received: 15 November 2025; Accepted: 9 March 2026;
Published online: 25 March 2026

References

1. Haumont, M. et al. Neutralizing antibody responses induced by varicella-zoster virus gE and gB glycoproteins following infection, reactivation or immunization. *J. Med. Virol.* **53**, 63–68 (1997).
2. Asada, H. VZV-specific cell-mediated immunity, but not humoral immunity, correlates inversely with the incidence of herpes zoster and the severity of skin symptoms and zoster-associated pain: The SHEZ study. *Vaccine* **37**, 6776–6781 (2019).
3. Levin, M. J. et al. Varicella-zoster virus-specific immune responses in elderly recipients of a herpes zoster vaccine. *J. Infect. Dis.* **197**, 825–835 (2008).
4. Good, R. A. & Zak, S. J. Disturbances in gamma globulin synthesis as experiments of nature. *Pediatrics* **18**, 109–149 (1956).
5. Hayashida, K. et al. Evaluation of varicella zoster virus-specific cell-mediated immunity by using an interferon-gamma enzyme-linked immunosorbent assay. *J. Immunol. Methods* **426**, 50–55 (2015).
6. Banovic, T. et al. Disseminated varicella infection caused by varicella vaccine strain in a child with low invariant natural killer T cells and diminished CD1d expression. *J. Infect. Dis.* **204**, 1893–1901 (2011).
7. Etzioni, A. et al. Fatal varicella associated with selective natural killer cell deficiency. *J. Pediatr.* **146**, 423–425 (2005).
8. Levy, O. et al. Disseminated varicella infection due to the vaccine strain of varicella-zoster virus, in a patient with a novel deficiency in natural killer T cells. *J. Infect. Dis.* **188**, 948–953 (2003).
9. Vossen, M. T. et al. Absence of circulating natural killer and primed CD8+ cells in life-threatening varicella. *J. Infect. Dis.* **191**, 198–206 (2005).
10. Goldblatt, D., Alter, G., Crotty, S. & Plotkin, S. A. Correlates of protection against SARS-CoV-2 infection and COVID-19 disease. *Immunol. Rev.* **310**, 6–26 (2022).
11. Richardson, S. I. et al. SARS-CoV-2 Omicron triggers cross-reactive neutralization and Fc effector functions in previously vaccinated, but not unvaccinated, individuals. *Cell Host Microbe* **30**, 880–886.e884 (2022).
12. Dufloo, J. et al. Asymptomatic and symptomatic SARS-CoV-2 infections elicit polyfunctional antibodies. *Cell Rep. Med* **2**, 100275 (2021).
13. Felber, B. K. et al. Co-immunization of DNA and protein in the same anatomical sites induces superior protective immune responses against SHIV challenge. *Cell Rep.* **31**, 107624 (2020).
14. Keshwara, R. et al. A recombinant Rabies virus expressing the Marburg virus glycoprotein is dependent upon antibody-mediated cellular cytotoxicity for protection against Marburg virus disease in a murine model. *J. Virol.* **93**, e01865–01818 (2019).
15. Chen, D. et al. Reduced neutralization and Fc effector function to Omicron subvariants in sera from SARS-CoV-1 survivors after two doses of CoronaVac plus one dose subunit vaccine. *J. Med. Virol.* **95**, e29136 (2023).
16. Bouayad, A. Multifaceted roles of Fcgamma receptors in COVID-19 and vaccine responses. *Am. J. Transl. Res* **15**, 3040–3059 (2023).
17. Diez, J. M. et al. Anti-severe acute respiratory syndrome coronavirus 2 hyperimmune immunoglobulin demonstrates potent neutralization and antibody-dependent cellular cytotoxicity and phagocytosis through N and S proteins. *J. Infect. Dis.* **225**, 938–946 (2022).
18. Park, S. Y. et al. Development of antibody-dependent cellular cytotoxicity in response to recombinant and live-attenuated herpes zoster vaccines. *NPJ Vaccines* **7**, 123 (2022).
19. Zhang, Y., Hoppe, A. D. & Swanson, J. A. Coordination of Fc receptor signaling regulates cellular commitment to phagocytosis. *Proc. Natl. Acad. Sci. USA.* **107**, 19332–19337 (2010).
20. Watzl, C. & Long, E. O. Signal transduction during activation and inhibition of natural killer cells. *Curr. Protoc. Immunol. Chapter* **11**, 11–19B (2010).
21. Petro, C. D. et al. HSV-2 DeltagD elicits FcgammaR-effector antibodies that protect against clinical isolates. *JCI Insight* **1**, e88529 (2016).
22. Dias, A. G. Jr. et al. Antibody Fc characteristics and effector functions correlate with protection from symptomatic dengue virus type 3 infection. *Sci. Transl. Med.* **14**, eabm3151 (2022).
23. Zohar, T. et al. Upper and lower respiratory tract correlates of protection against respiratory syncytial virus following vaccination of nonhuman primates. *Cell Host Microbe* **30**, 41–52.e45 (2022).
24. Bartsch, Y. C. et al. Antibody effector functions are associated with protection from respiratory syncytial virus. *Cell* **185**, 4873–4886.e4810 (2022).
25. Richardson, S. I. et al. SARS-CoV-2 Beta and Delta variants trigger Fc effector function with increased cross-reactivity. *Cell Rep. Med.* **3**, 100510 (2022).
26. Geers, D. et al. Ad26.COV2.S priming provided a solid immunological base for mRNA-based COVID-19 booster vaccination. *iScience* **26**, 105753 (2023).

27. Adeniji, O. S. et al. COVID-19 severity is associated with differential antibody Fc-mediated innate immune functions. *mBio* **12**, e00281–00221 (2021).
28. Paquin-Proulx, D. et al. Associations between antibody Fc-mediated effector functions and long-term sequelae in Ebola virus survivors. *Front. Immunol.* **12**, 682120 (2021).
29. Henry Dunand, C. J. et al. Both neutralizing and non-neutralizing human H7N9 influenza vaccine-induced monoclonal antibodies confer protection. *Cell Host Microbe* **19**, 800–813 (2016).
30. Richardson, S. I. et al. IgG3 enhances neutralization potency and Fc effector function of an HIV V2-specific broadly neutralizing antibody. *PLoS Pathog.* **15**, e1008064 (2019).
31. Sundqvist, V. A., Linde, A. & Wahren, B. Virus-specific immunoglobulin G subclasses in herpes simplex and varicella-zoster virus infections. *J. Clin. Microbiol.* **20**, 94–98 (1984).
32. Lee, Y. H. et al. Global varicella vaccination programs. *Clin. Exp. Pediatr.* **65**, 555–562 (2022).
33. Kawai, K., Gebremeskel, B. G. & Acosta, C. J. Systematic review of incidence and complications of herpes zoster: towards a global perspective. *BMJ Open* **4**, e004833 (2014).
34. de Jong, M. D., Weel, J. F., Schuurman, T., Wertheim-van Dillen, P. M. & Boom, R. Quantitation of varicella-zoster virus DNA in whole blood, plasma, and serum by PCR and electrochemiluminescence. *J. Clin. Microbiol.* **38**, 2568–2573 (2000).
35. Arvin, A. M., Moffat, J. F. & Redman, R. Varicella-zoster virus: aspects of pathogenesis and host response to natural infection and varicella vaccine. *Adv. Virus Res.* **46**, 263–309 (1996).
36. Burel, J. G., Apte, S. H., Groves, P. L., McCarthy, J. S. & Doolan, D. L. Polyfunctional and IFN-gamma monofunctional human CD4(+) T cell populations are molecularly distinct. *JCI Insight* **2**, e87499 (2017).
37. Freen-van Heeren, J. J. et al. Assessing antigen-specific T cell responses through IFN-gamma Enzyme-Linked Immune Absorbent Spot (ELISpot). *Methods Mol. Biol.* **2782**, 209–226 (2024).
38. Laing, K. J. et al. Zoster vaccination increases the breadth of CD4+ T cells responsive to varicella zoster virus. *J. Infect. Dis.* **212**, 1022–1031 (2015).
39. Weinberg, A. et al. Varicella-zoster virus-specific cellular immune responses to the live attenuated zoster vaccine in young and older adults. *J. Immunol.* **199**, 604–612 (2017).
40. Cunningham, A. L. et al. Immune responses to a recombinant glycoprotein E herpes zoster vaccine in adults aged 50 years or older. *J. Infect. Dis.* **217**, 1750–1760 (2018).
41. Asanuma, H., Sharp, M., Maecker, H. T., Maino, V. C. & Arvin, A. M. Frequencies of memory T cells specific for varicella-zoster virus, herpes simplex virus, and cytomegalovirus by intracellular detection of cytokine expression. *J. Infect. Dis.* **181**, 859–866 (2000).
42. Atyeo, C. et al. Distinct early serological signatures track with SARS-CoV-2 survival. *Immunity* **53**, 524–532.e524 (2020).
43. Barouch, D. H. et al. Protective efficacy of a global HIV-1 mosaic vaccine against heterologous SHIV challenges in rhesus monkeys. *Cell* **155**, 531–539 (2013).
44. Richardson, S. I. et al. HIV-specific Fc effector function early in infection predicts the development of broadly neutralizing antibodies. *PLoS Pathog.* **14**, e1006987 (2018).
45. Ullah, I. et al. Live imaging of SARS-CoV-2 infection in mice reveals that neutralizing antibodies require Fc function for optimal efficacy. *Immunity* **54**, 2143–2158.e2115 (2021).
46. Winkler, E. S. et al. Human neutralizing antibodies against SARS-CoV-2 require intact Fc effector functions for optimal therapeutic protection. *Cell* **184**, 1804–1820.e1816 (2021).
47. Zohar, T. et al. Compromised humoral functional evolution tracks with SARS-CoV-2 mortality. *Cell* **183**, 1508–1519.e1512 (2020).
48. Ihara, T. et al. Antibody response determined with antibody-dependent cell-mediated cytotoxicity (ADCC), neutralizing antibody, and varicella skin test in children with natural varicella and after varicella immunization. *Acta Paediatr. Jpn.* **33**, 43–49 (1991).
49. Asano, Y. et al. Immunoglobulin subclass antibodies to varicella-zoster virus. *Pediatrics* **80**, 933–936 (1987).
50. Jounai, N. et al. Age-specific profiles of antibody responses against respiratory syncytial virus infection. *EBioMedicine* **16**, 124–135 (2017).
51. Bruhns, P. Properties of mouse and human IgG receptors and their contribution to disease models. *Blood* **119**, 5640–5649 (2012).
52. Chung, A. W. et al. Polyfunctional Fc-effector profiles mediated by IgG subclass selection distinguish RV144 and VAX003 vaccines. *Sci. Transl. Med.* **6**, 228–238 (2014).
53. Lim, J., Kim, Y., Hwang, J. Y., Lee, K. M. & Park, H. Evaluation of flow cytometry-based fluorescent antibody to membrane antigen test to measure the humoral immunity against the varicella-zoster virus. *Heliyon* **10**, e36614 (2024).
54. Pollara, J. et al. Application of area scaling analysis to identify natural killer cell and monocyte involvement in the GranToxiLux antibody dependent cell-mediated cytotoxicity assay. *Cytom. A* **93**, 436–447 (2018).
55. Parekh, B. S. et al. Development and validation of an antibody-dependent cell-mediated cytotoxicity-reporter gene assay. *MAbs* **4**, 310–318 (2012).
56. Yang, F. et al. Validation of an IFN-gamma ELISpot assay to measure cellular immune responses against viral antigens in non-human primates. *Gene Ther.* **29**, 41–54 (2022).
57. Butler, A. L., Fallon, J. K. & Alter, G. A Sample-Sparing Multiplexed ADCP Assay. *Front. Immunol.* **10**, 1851 (2019).
58. European Medicines, A. ICH Q2(R2) Validation of analytical procedures scientific guideline. (2023).
59. Raimo, M., Zavoianu, A. G., Meijs, W., Scholten, P. & Spanholtz, J. Qualification of a flow cytometry-based method for the evaluation of in vitro cytotoxicity of GTA002 natural killer cell therapy. *Heliyon* **10**, e24715 (2024).
60. Hwang, J. Y. et al. Cross-reactive humoral immunity of clade 2 Oka and MAV/06 strain-based varicella vaccines against different clades of varicella-zoster virus. *Hum. Vaccin. Immunother.* **19**, 2210961 (2023).

Acknowledgements

This study was supported by grant 23202MFDS136 (2023) from the Ministry of Food and Drug Safety, Republic of Korea. The funding agency had no role in the study design; data collection, analysis, or interpretation; manuscript preparation; or the decision to publish.

Author contributions

S.X., J.Y.H., H.S.L., O.S.S., J.Y.N., S.H.H., and H.P. conceived and designed the study. S.X., J.Y.H., Y.K., K.M.L., E.J.J., S.T.C., J.S.L., J.Y.B., K.K., B.Y., and J.H.L. performed the experiments and collected the data. S.X. and Y.K. analyzed the data. S.X., J.Y.H., Y.K., and H.P. drafted the manuscript, which was critically reviewed by all authors.

Competing interests

The authors declare no competing interests.

Additional information

Supplementary information The online version contains supplementary material available at https://doi.org/10.1038/s41541-026-01424-w.

Correspondence and requests for materials should be addressed to Hosun Park.

Reprints and permissions information is available at http://www.nature.com/reprints

Publisher's note Springer Nature remains neutral with regard to jurisdictional claims in published maps and institutional affiliations.

Open Access This article is licensed under a Creative Commons Attribution-NonCommercial-NoDerivatives 4.0 International License, which permits any non-commercial use, sharing, distribution and reproduction in any medium or format, as long as you give appropriate credit to the original author(s) and the source, provide a link to the Creative Commons licence, and indicate if you modified the licensed material. You do not have permission under this licence to share adapted material derived from this article or parts of it. The images or other third party material in this article are included in the article's Creative Commons licence, unless indicated otherwise in a credit line to the material. If material is not included in the article's Creative Commons licence and your intended use is not permitted by statutory regulation or exceeds the permitted use, you will need to obtain permission directly from the copyright holder. To view a copy of this licence, visit http://creativecommons.org/licenses/by-nc-nd/4.0/.

© The Author(s) 2026